M.O.11 Technical Note Number 16.

A semi-Lagrangian Method applied to baretropic forecasts at 500mb.

By J. S. Sawyer and J. Pertnall.

1. Introduction

In a previous paper (Sawyer, 1960) a semi-Lagrangian method was proposed for the solution of the vorticity advection equation and its advantages demonstrated on analytical fields used to represent 500mb height distributions. The present paper reports the application of a similar computing technique to ten real 500mb height distributions. The first calculations revealed that the procedures developed on the analytical fields led to substantial errors when applied to practical forecasting mainly as a result of inadequate representation of the vorticity advected into the computing area across the inflow boundary, but also on account of the irregular grouping of the points to which vorticity values were attached and which were traced during the computation. The procedure outlined in section 2 incorporates modifications necessary to overcome these difficulties.

The semi-Lagrangian procedure leads to forecasts of similar accuracy to those obtained by the more usual Eulerian method and permits a time-step of 6 hours. Significant differences between the two solutions arise. Some of these are attributable to the different treatment of boundary conditions but others can be associated with truncation errors to be expected in the Eulerian solution.

2. Method of computation

Both the experimental semi-Lagrangian forecasts and the Eulerian computations used for comparison were carried out on a flow represented by a stream function, ψ, which had been determined from the field of 500mb height, h, by the solution of the balance equation, as suggested by Charney (1955). The balance equation was solved in the form

$$2\left\{\frac{\partial^2\psi}{\partial x^2}\cdot\frac{\partial^2\psi}{\partial y^2}-\left(\frac{\partial^2\psi}{\partial x\,\partial y}\right)^2\right\}+f\nabla^2\psi+\frac{\partial\psi}{\partial x}\frac{\partial f}{\partial x}+\frac{\partial\psi}{\partial y}\frac{\partial f}{\partial y}=g\nabla^2 h \qquad \text{-------(1)}$$

/The

The method followed that of Miyakoda (1960) and the procedure is described by Jones (1962).

At the completion of the integration for ψ with respect to time the field of 500mb height was reconstructed by solving equation (1) as a Poisson equation for h in terms of ψ assuming that the boundary values of h were unchanged.

The vorticity advection equation which is the basis of the barotropic model for numerical forecasting is

$$\frac{\partial \eta}{\partial t} + J(\psi, \eta) = 0 \qquad \text{--------(2)}$$

where

$$\eta = \nabla^2 \psi + f \qquad \text{--------(3)}$$

and f is the Coriolis parameter. These equations pose exactly the same problem as treated in the experiments on analytical fields (Sawyer, 1960) and were solved in a similar manner. They correspond to the advection of the absolute vorticity, η, by a wind field given by $\underset{\sim}{V} = \underset{\sim}{k} \times \nabla\psi$

The steps taken in the course of the semi-Lagrangian method of integration may be summarised as follows:-

(i) Form a list of fluid elements and list the associated absolute vorticity, η, calculated from the initial stream function, ψ.

(ii) Calculate the advecting field, $\underset{\sim}{V}$, from ψ.

(iii) Interpolate $\underset{\sim}{V}$ to the positions of the fluid elements.

(iv) Calculate the displacements of the fluid elements and their new positions after one time step.

(v) Delete from the list of fluid elements those leaving the area of the computation grid, and add to the list additional elements to represent the vorticity of the air entering the area.

(vi) Form the field of relative vorticity, $J (= \nabla^2 \psi)$, from the absolute vorticity of the fluid elements $\eta (= J + f)$.

(vii) Calculate the stream function, ψ, from the new vorticity field, J.

(viii) Repeat from step (ii).

The calculations were carried out using a 24 X 20 rectangular grid covering the North Atlantic and Europe as used in numerical forecasting experiments by

/Knighting

Knighting and others (1960).

The procedure closely followed that of Sawyer (1960) except at step (vi) and is given in more detail below. The following notation is used:-

∇^2 is the finite difference approximation to the operator ∇^2. Thus $\nabla^2\psi = \frac{1}{h^2}\{\psi_1 + \psi_2 + \psi_3 + \psi_4 - 4\psi_0\}$ where h is the grid-length and ψ_0, ψ_1 etc. are the values of the stream function, ψ, at an array of points as arranged in Fig. 1.

η_r is the finite difference approximation to the vorticity of the r^{th} fluid element at its initial position.

T is the time-step.

Step 1: The initial list of fluid elements contained one entry for each point of the basic grid, excluding boundary points[1]. With each fluid element was associated its initial absolute vorticity which remained unaltered during the calculation. This was calculated from the simple finite difference approximation

$$\eta_r = \{\nabla^2\psi\}_{t=0} + f \qquad \text{--------(4)}$$

Step 2: Following Fjørtoft (1955) and Wiin-Nielsen (1959) advection was carried out using winds derived from a smoothed stream function, ψ', where (in the notation of Fig. 1)

$$\psi_0' = \frac{1}{4}(\psi_1 + \psi_2 + \psi_3 + \psi_4) \qquad \text{--------(5)}$$

Advecting velocities at grid points were calculated using simple two-point finite differences (centred differences were used except at boundary points where one-sided differences were necessary).

At interior points

$$\left.\begin{aligned} u_0' &= -\frac{1}{2h}(\psi_2' - \psi_4') \\ v_0' &= \frac{1}{2h}(\psi_1' - \psi_3') \end{aligned}\right\} \text{--------(6)}$$

Step 3: After the initial time-step the fluid elements are to be found, not at grid points, but within the squares which form the mesh. Interpolation of the wind components u' and v' to the position P(r,s) of the fluid element within

/a

Footnote 1. If the vorticity exceeded the capacity of representation by a ten-bit number in the computer, the vorticity was divided between two points with identical coordinates.

square was carried out by means of the formula

$$g_P = (1-s)\{(1-r)g_0 + rg_1\} + s\{(1-r)g_2 + rg_3\} \qquad \text{------(7)}$$

Suffices refer to positions in Figure 2 and g may represent either u' or v'.

Step 4: At each time step except the first, the value of the coordinates of each fluid element for use at the next time step were calculated from the centred difference relations

$$\left.\begin{aligned} X'_{t+1} &= X_{t-1} + 2u'_t T \\ Y'_{t+1} &= Y_{t-1} + 2v'_t T \end{aligned}\right\} \text{-----(8)}$$

where X' and Y' are preliminary values for use at the next time step. The value of X'_t was, however, subsequently corrected when u'_t had been calculated to give an improved value.

$$\left.\begin{aligned} X_t &= X_{t-1} + \tfrac{1}{2}(u'_t + u'_{t-1})T \\ \text{similarly} \quad Y_t &= Y_{t-1} + \tfrac{1}{2}(v'_t + v'_{t-1})T \end{aligned}\right\} \text{------(9)}$$

At the first time step uncentred differences were used in place of (9).

Thus

$$\left.\begin{aligned} X_1' &= X_0 + u_0' T \\ Y_1' &= Y_0 + v_0' T \end{aligned}\right\} \text{------(10)}$$

The computing programme also contained facilities to repeat the second time step[2], so that estimates of u'_1 and v'_1 could be included in the computation of the positions of the fluid elements at the end of the first time step by means of equations (9) before the computation proceeded. This was expected to reduce the error introduced by the first uncentred time step and the modification was used in the experiments described in later sections.

Step 5: All fluid elements with new coordinates outside the boundary of the grid were deleted from the list before the computation proceeded.

The results of the baroтropic forecasts were found to be sensitive to the procedure adopted for introducing new fluid elements at inflow boundaries and several variants were tried. The procedure found most successful (adopted in

/programme

---

[2] Footnote. In programme BIL a hand-switch setting of 0 results in no repeat of the second time step; a setting of 1 repeats the second step.

programme BIL (I)) was as follows. The inflow velocity normal to the boundary, v_n, was computed at the first interior row of points from the stream function at the initial stage. New fluid elements were introduced at time step, n, if $v_n nT/h$ had increased beyond a new integer since time step, n - 1, (thus new fluid elements were introduced every time a fluid element moving inwards with the normal velocity v_n would have crossed a grid line parallel to the boundary). The vorticity attributed to the new fluid element was the vorticity of the initial field at the point from which it was initiated. If $v_n nT/h$ increased past two or more integral values in one time step, two or more new fluid elements were introduced at points appropriately displaced into the computation area along the initial wind vector at the inflow point.

Step 6: The procedure adopted to reconstruct the distribution of vorticity from the list of fluid elements was modified from that adopted by Sawyer (1960) because on some occasions fictitious concentrations of the fluid elements arose from truncation error in the flow which should have been non-divergent. The procedure was therefore based on the average vorticity of the fluid elements in the neighbourhood of each grid point (rather than on the total vorticity on the fluid elements in the neighbourhood) but steps were also taken to conserve the total vorticity within the computation area. In detail the procedure was as follows.

(a) For each fluid element, for example at point P in Fig 2, the absolute vorticity η is allocated to the corner points 0, 1, 2 and 5 of the square in which it lies by multiplying by (1 - r)(1 - s), r(1 - s), (1 - r)s and rs respectively. Subsequently the vorticity appropriate to each grid point is determined from $\eta_P = \bar{f} + \left[\sum_n a_n(\eta - \bar{f})\right] \Big/ \sum_n a_n$ where the summation is over all the fluid elements in the squares surrounding P and a_n represents the factor by which the vorticity of the fluid element has been multiplied. ($\bar{f}$ is the average value of the Coriolis parameter over the area).

(b) If $\sum_n a_n = 0$ a mean value, M, of η_P at surrounding grid points is substituted.

(c) The total loss or gain of vorticity within the field is computed and shared equally among grid points to conserve the total. The quantity which has

/to

to be thus shared is

$$A = \sum_{\substack{\text{over all points} \\ \text{for which} \\ n \neq 0}} \left[\left\{ \sum_n a_n (\eta - \bar{f}) \right\} \left(1 - \frac{1}{\sum a_n} \right) \right] - \sum_{\substack{\text{over all points} \\ \text{for which} \\ m = 0}} M$$

(d) The value of the relative vorticity is computed from

$$f_p = \eta_p - f$$

Step 7: The new field of the stream function ψ_t is calculated from the field of relative vorticity from the equation

$$\nabla^2 \psi_t = \mathcal{J}_p \qquad \text{--------(11)}$$

which is solved by the usual iterative Liebmann process. Linear extrapolation with respect to time is used to produce a first guess for ψ_t after the second time-step and over-relaxation by a factor of 4/3 is employed. Boundary values of ψ_t were maintained unchanged. Twenty iterations were found adequate at each time step.

3. Results

Barotropic forecasts have been carried out for the 500mb level on ten synoptic situations using the programme (BIL(I)) on METEOR designed to employ the semi-Lagrangian method described in Section 2. Results of similar barotropic forecasts for these occasions were available from the programme (BIX) which uses the conventional finite difference method of solving equations (2) and (3). Some statistics of the results are contained in Table I. These statistics apply to an inner area of 16 X 12 as illustrated in Figures 3 and 4. The semi-Lagrangian forecasts were all made with a time step of 6 hours. The distributions of the mean error and r.m.s. error over the inner verification area are shown for the two techniques in Figs 3 and 4.

Interesting differences were found between the two sets of forecasts and these are discussed in more detail in the following paragraphs. Some of the differences were large enough to materially affect the interpretation to be set on the chart in terms of the weather of some areas. Overall there is little to

/choose

choose between the statistics of success of the two methods, except that the r.m.s. height error does tend to be larger when the semi-Lagrangian method is used. However, the correlation coefficient between predicted and observed changes is slightly higher with the semi-Lagrangian method.

The error distributions in the forecasts computed by the two methods are essentially similar in their large-scale features, this common part of the error field arising, presumably, from the deficiencies of the barotropic model. Differences between the two sets of forecasts arise in two ways:- (a) from the difference in the boundary conditions used in the two computing techniques and (b) from differences in the approximation to the solution of equation (2). To some extent these two effects can be distinguished and will be considered separately below.

4. Errors arising from boundary conditions

In both the semi-Lagrangian and conventional Eulerian techniques the boundary values of the 500mb height and stream function, ψ , are retained unchanged during the integration with respect to time. However an additional condition is needed where air is entering the area. In the Eulerian technique this is provided by the assumption that the stream function, ψ , is unchanged at the first interior row of the mesh. This condition is applied at both inflow and outflow points and the problem is overspecified at the latter. In the semi-Lagrangian technique the second boundary condition is provided by specifying the vorticity of the inflowing air as equal to the initial vorticity.

All of these assumptions are false and introduce errors into the forecasts.

At the inflow boundary the errors introduced into the two methods are rather similar. This is understandable when it is realised that at the western boundary in the Eulerian method the vorticity at the first interior row is evaluated from ψ at five points arranged as in Fig. 1 at four of which ψ remains fixed. Thus in the vorticity attributed to this point, $\frac{1}{h^2}(\psi_1 + \psi_2 + \psi_3 + \psi_4 - 4\psi_0)$, only ψ_1 varies and the procedure corresponds to the advection across the boundary of vorticity containing a large element of the initial vorticity. However there are differences between the solutions by the two methods which extend

/some

some distance inwards from the inflow boundary. This is illustrated by the extreme case of 16 February 1959, Figs. 5(a) - (d) in which the semi-Lagrangian forecast had much larger errors than the Eulerian forecast. These arose very largely from the western boundary on which there was strong cyclonic vorticity on the initial chart. Both methods advected the vorticity into the area and formed a trough which was too intense and too far south, but the effect was more serious in the Lagrangian method in which the full vorticity advection was maintained throughout the forecast. In fact the trough line moved into the area and the cyclonic advection was replaced by the advection of anticyclonic vorticity on the boundary during the period.

Apart from this one bad case the relative magnitudes of the inflow boundary errors in the two techniques seems to be largely fortuitous with perhaps some tendency for the errors of the semi-Lagrangian forecasts to be smaller. A simpler semi-Lagrangian scheme in which air entering the area was assumed to have zero relative vorticity suffered much larger errors than both the scheme described in Section 2 and the Eulerian method.

At the outflow boundary the overspecification of the boundary conditions leads to considerable irregularity in the Eulerian forecasts in the rows adjacent to the boundary. This effect does not arise in the semi-Lagrangian forecasts which are entirely smooth. Boundary errors of this type can be seen in the upper right of Fig. 5(d) (Eulerian forecast) but do not appear in the corresponding semi-Lagrangian forecast Fig. 5(c).

5. Truncation errors

From the calculation upon artificial stream functions represented by analytical forms (Sawyer, 1960) it would be expected that computations using the Lagrangian method would lead to higher speeds for pressure troughs, ridges and centres than would the conventional finite difference calculations. This is an effect of truncation error in the usual formulation of the Eulerian scheme. Such an effect does not appear strongly in the available series of forecasts for which the computed displacements by the two methods are compared in Table II. Only in respect of the ridges, which were generally fast moving features, is the

/difference

difference apparent.

Table II - Average computed displacements of isobaric features.

	Mean displacement (n.m)			No. of examples
	Calculated BIL(I) Semi-Lagrangian	Calculated BIS Conventional finite-differences	Actual	
Lows	332	330	318	12
Troughs	230	230	230	1
Highs	280	270	213	3
Ridges	512	437	427	4

A noteworthy difference in the computed displacement of "lows" by the two methods was however noted. This is a tendency for the conventional finite difference method to lead to a track to the right of that predicted by the semi-Lagrangian method. The same effect was found in the computations on analytical forms (Sawyer, 1960) and was then attributed to the distortion of the profile of the stream function through the "low" as a result of truncation error; this tends to build up large wind velocities in the rear of the low and leads to an erroneous displacement to the right.

In general the position of isobaric features predicted by the semi-Lagrangian method appeared to be better than that of the Eulerian method. It was classed as better in respect of 11 features, as good for 5 features and worse for 4.

A particularly interesting case is that of forecasts based on the situation at 0000 G.M.T. on 27 October 1959, and is illustrated in Figs. 6(a) - (d). The movement of a depression across the British Isles was predicted as SSE-ward by the conventional finite difference method, but the actual movement was ESE-ward and this was correctly given by the semi-Lagrangian method. There were no important differences between the two forecasts in other areas of the chart and the difference in the treatment of the depression must have arisen almost entirely from the truncation errors of the finite difference method. The tendency for the finite difference method to displace the centres of depressions to the right

/of

of their proper track has already been remarked.

Another case of a deep depression which was treated differently by the two techniques was that of 16 January 1959. A very deep depression was predicted by the finite difference method to extend eastward leading to a considerable fall in 500mb height to the east of the centre. The semi-Lagrangian method predicted a greater movement of the centre accompanied by filling and less trough extension to the east. The semi-Lagrangian method was considerably more successful in this case but this may have been fortuitous as boundary assumptions as well as truncation errors were involved. However, it is noteworthy that differences of up to 17dm arose between the two methods.

6. Dependance of the semi-Lagrangian forecasts on details of the technique

During the development of the semi-Lagrangian technique for integration several experiments were made to determine the most suitable length for the time step and other details of the procedure. Although it was subsequently found necessary to change the treatment of the boundary conditions and the method of solving the balance equation was also changed slightly, the conclusions derived from these experiments are likely to remain valid and are given below.

(a) Time-step A few forecasts were made with time steps of 3 hrs and 12 hrs as well as with the step of 6 hours which was regarded as standard. Only small differences (up to 4dm in height) arose from the change from 6 hour to 3 hour time steps, but larger and significant differences (up to 14dm) arose when the time step was increased to 12 hours. However, the computation remained stable.

In the example illustrated in Fig 5 a reduction in time-step to 1-hour resulted in larger changes (up to 18dm on the western edge of the verification area). This was almost certainly due to the treatment of the inflowing air by the shorter time step which was otherwise projected inward with its velocity on the boundary for 6 hours following a straight line instead of a more appropriate curved path.

(b) Repetition of the second time-step Two integrations were performed omitting the repetition of the second time step and thus relying on an uncentred

/difference

difference at the initial step. Differences were everywhere small - the maximum difference being 3dm. These forecasts were prepared in 6 hour steps, but differences were no greater in a forecast using 12 hour steps.

(c) Number of iterations in solving equation (11) The number of iterations to be used in solving equation (11) was fixed at 20 during these experiments. However, one integration was repeated with the number of iterations changed to 10. There was a small difference in the result in the centre of the chart with a maximum value of 2 to 3dm.

7. Discussion

The experiments show that the semi-Lagrangian technique described in section 2 is a practical method of integrating the barotropic prediction equation. There is no sign of computational instability even when the time step is extended to 12 hours. There seems little to be gained by reducing the time-step below 6 hours but forecasts with 12 hour time-steps suffer from locally significant truncation error.

There are significant differences between the results obtained by the semi-Lagrangian technique and the usual finite difference method. In part these may be attributed to differences in boundary procedure, but important differences can be attributed to truncation error in the usual finite difference procedure, particularly arising near to pressure centres.

Although the verification statistics of the semi-Lagrangian technique are not better than those of the Eulerian method, it provides a useful alternative which is suitable for monitoring computational errors and can be used to draw attention to some errors which arise in the mathematical procedure. The larger errors which are common to both computing procedures can be regarded as arising from the physical limitations of the barotropic model.

The semi-Lagrangian technique, being free from computational instability with time steps of several hours, may prove particularly well suited to barotropic forecasts over large areas, up to the hemisphere, for extended periods.

/References

References

Charney, J. G.	1955	Tellus, Vol 7, p.22.
Fjortoft, R.	1955	Tellus, Vol 7, p.462
Knighting, E., G. A. Corby, F.H. Bushby and C.E. Wallington	1961	London M.O. Sci. Pap. No 5.
Jones, D. E.	1962	Solution of balance equation as used in SIA programme - (Unpublished - enclosure 33A on M.O.11/45 Pt. 2).
Miyakoda, K.	1960	Tech Rep Jap. Met Agency No 3.
Sawyer, J.S.	1960	M.O.11 Tech Note (B) No 14.
Wiin-Nielsen, A.	1959	Tellus, Vol 11, p.180.

Table I Verification statistics for 24-hr 500mb barotropic forecasts prepared using a semi-Lagrangian method (BIL(I)) and a conventional finite difference method (BIX)

Date	Semi-Lagrangian BIL(I)			Finite-difference BIX			
	(a)	(b)	(c)	(a)	(b)	(c)	
12. 1. 59	68	25	0.42	93	30	0.09	
16. 1. 59	58	19	0.80	106	25	0.66	
5. 2. 59	54	24	0.82	56	25	0.80	
10. 2. 59	119	36	0.43	85	34	0.48	
16. 2. 59	132	30	0.79	72	20	0.92	
5. 3. 59	68	21	0.87	73	27	0.76	
20. 7. 59	43	13	0.88	30	13	0.87	
27. 7. 59	51	16	0.56	52	17	0.60	
10. 9. 59	57	21	0.75	52	18	0.80	
27.10. 59	86	21	0.89	73	24	0.86	
Mean	74	22.6	0.72	69	22.9	0.68	

(a) r.m.s. error in predicted 500mb height (metres)

(b) r.m.s. vector wind error (kts)

(c) correlation coefficient between observed and predicted 500mb height changes.

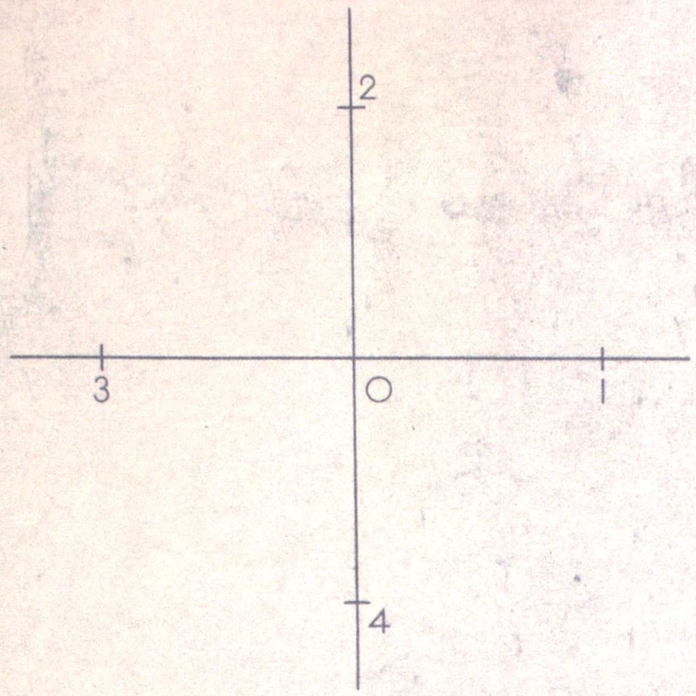

Fig. 1

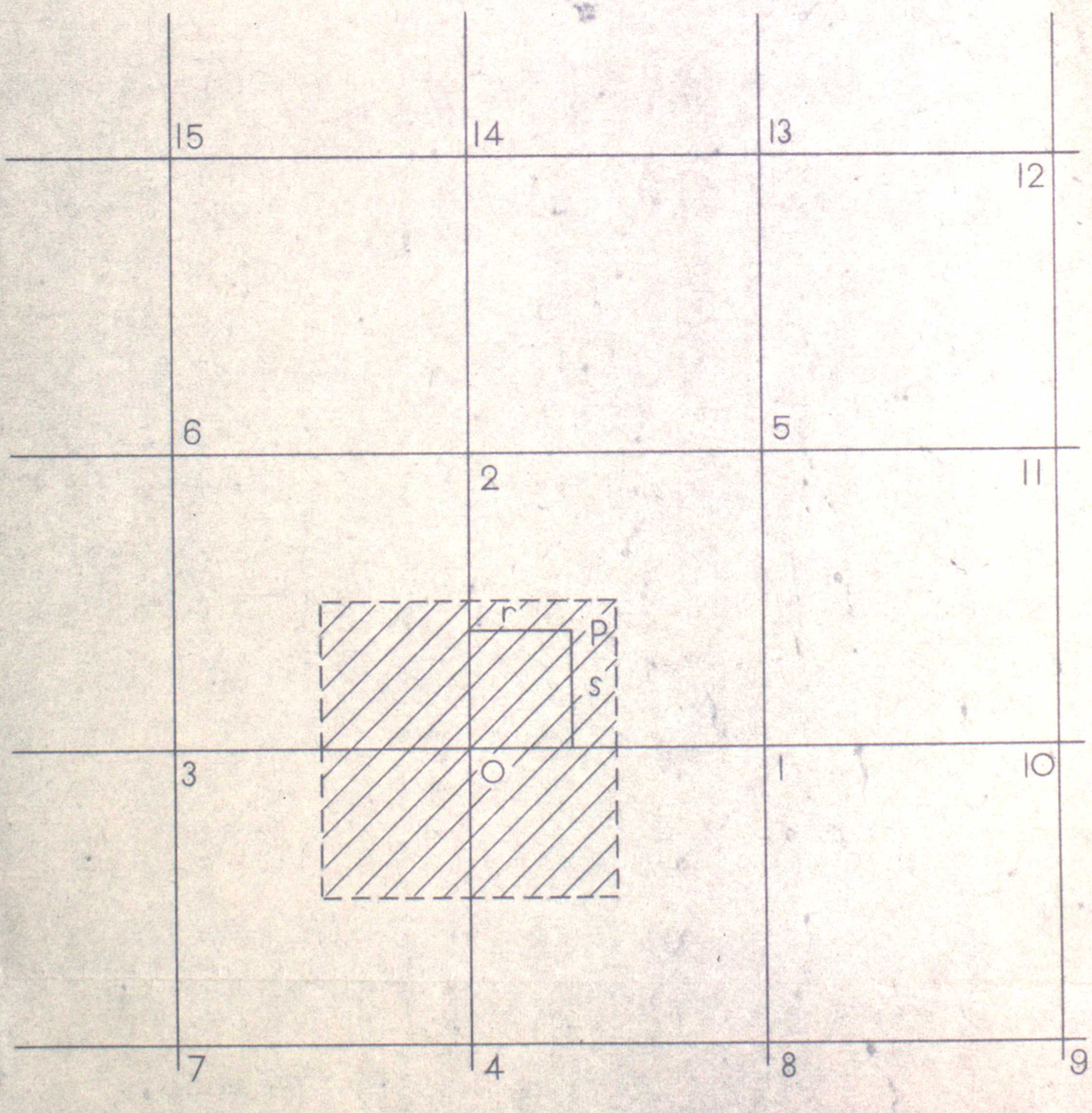

Fig. 2

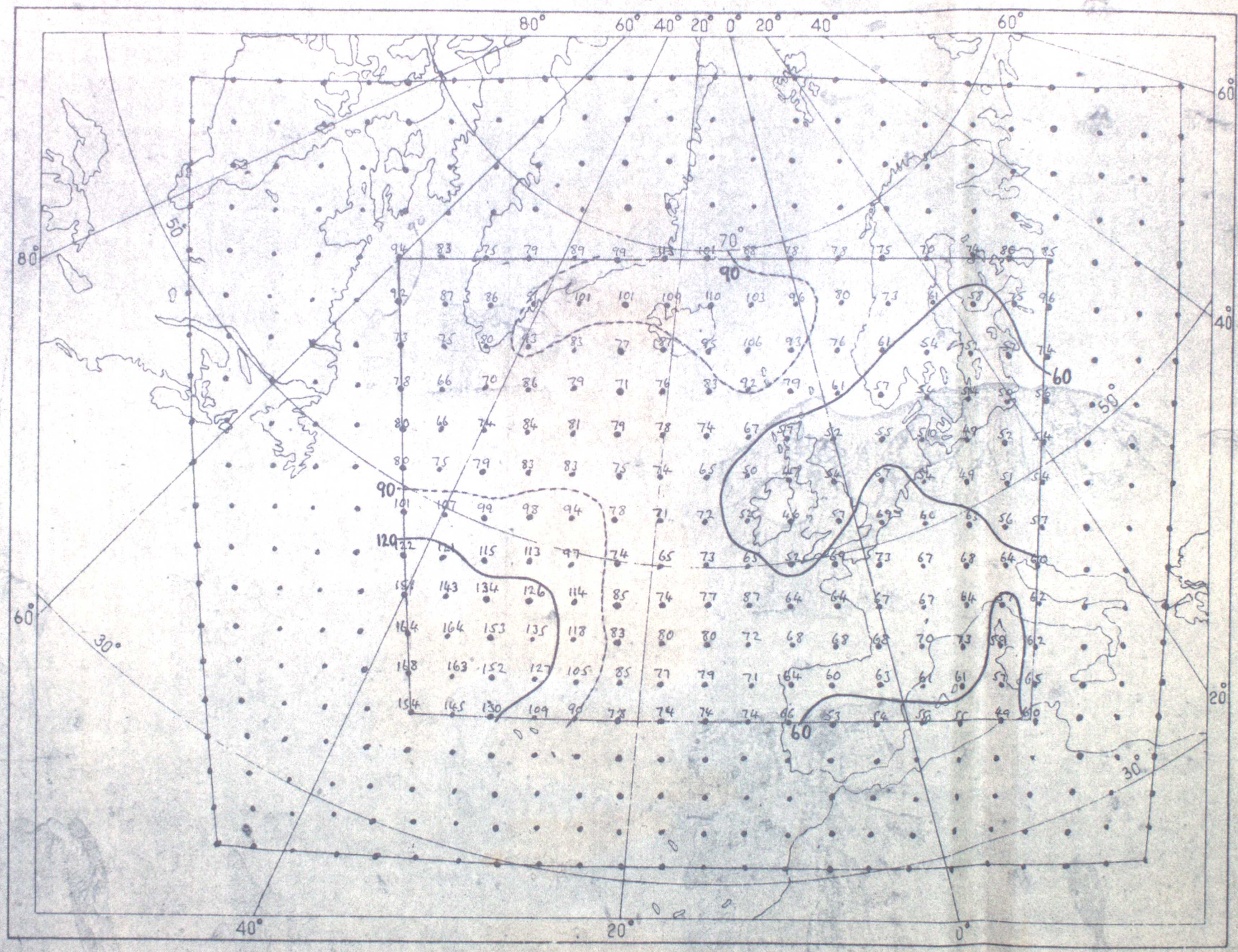

FIG 3 R.M.S. ERROR OF SEMI-LAGRANGIAN TECHNIQUE BIL (I) (METRES)

Printed by Air Ministry P.R.B.

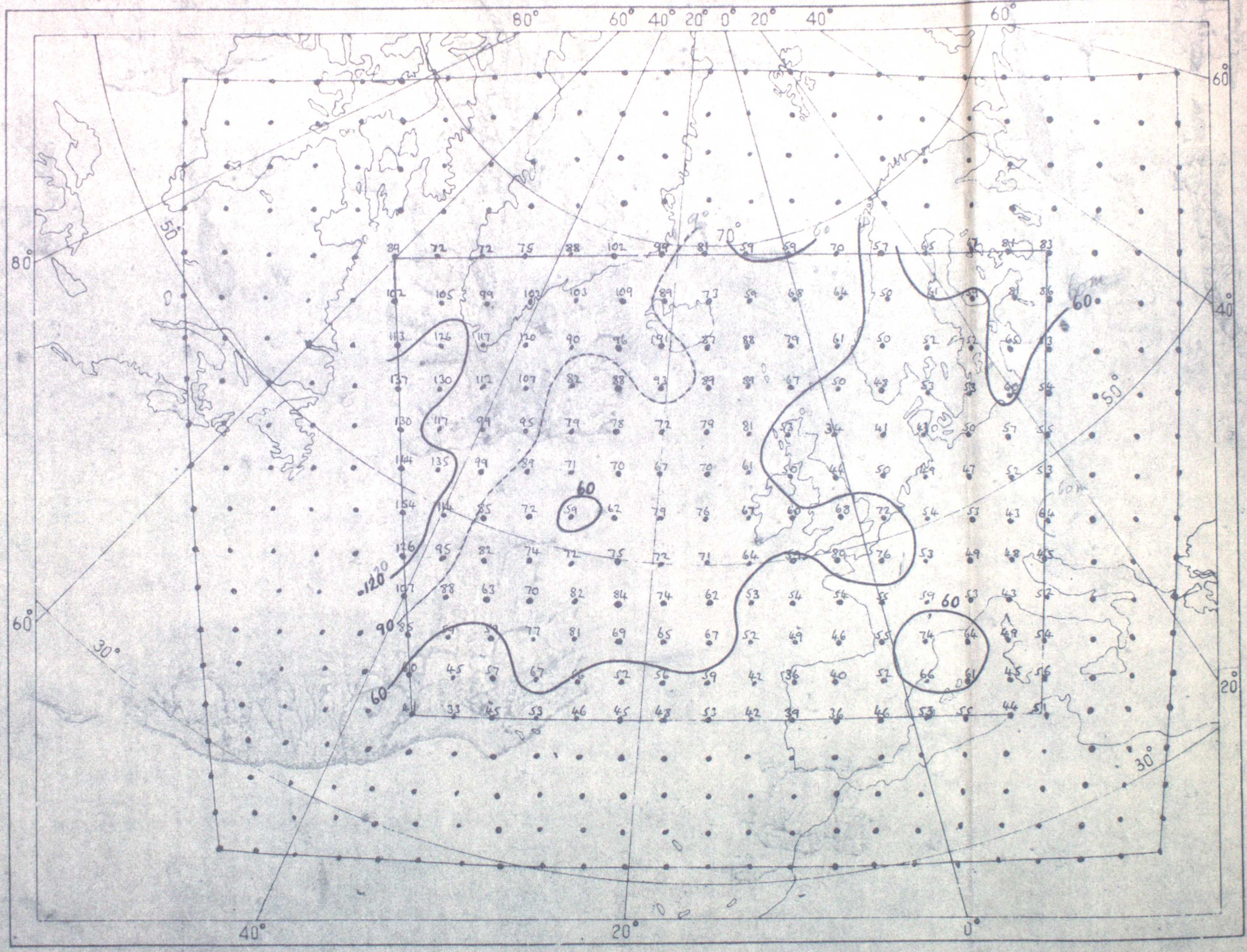

FIG 4 R.M.S. ERROR OF EULERIAN TECHNIQUE BIX (METRES)

Printed by Air Ministry P.R.B.

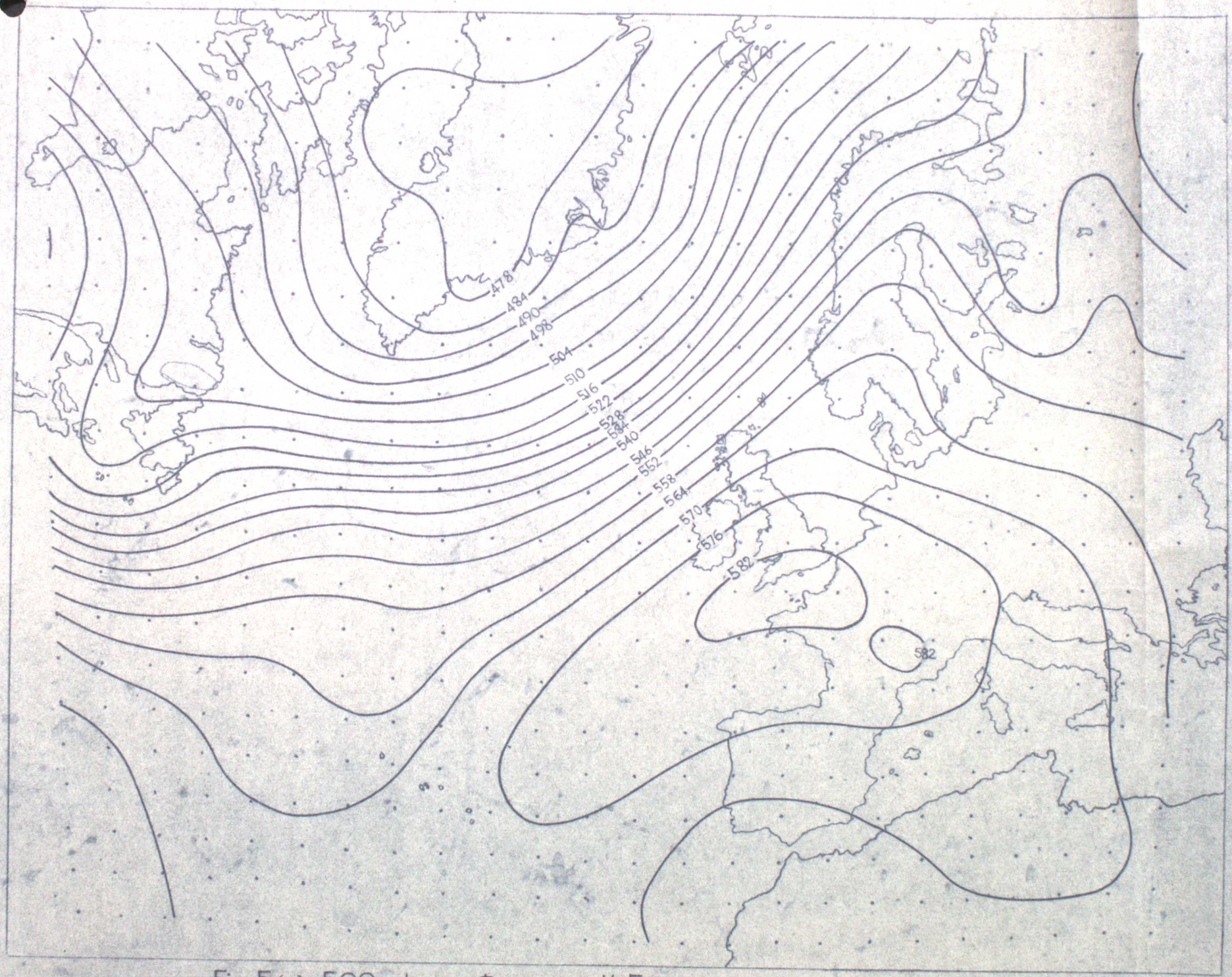

Fig. 5 (a) 500 mb. contours 16 Feb. 1959

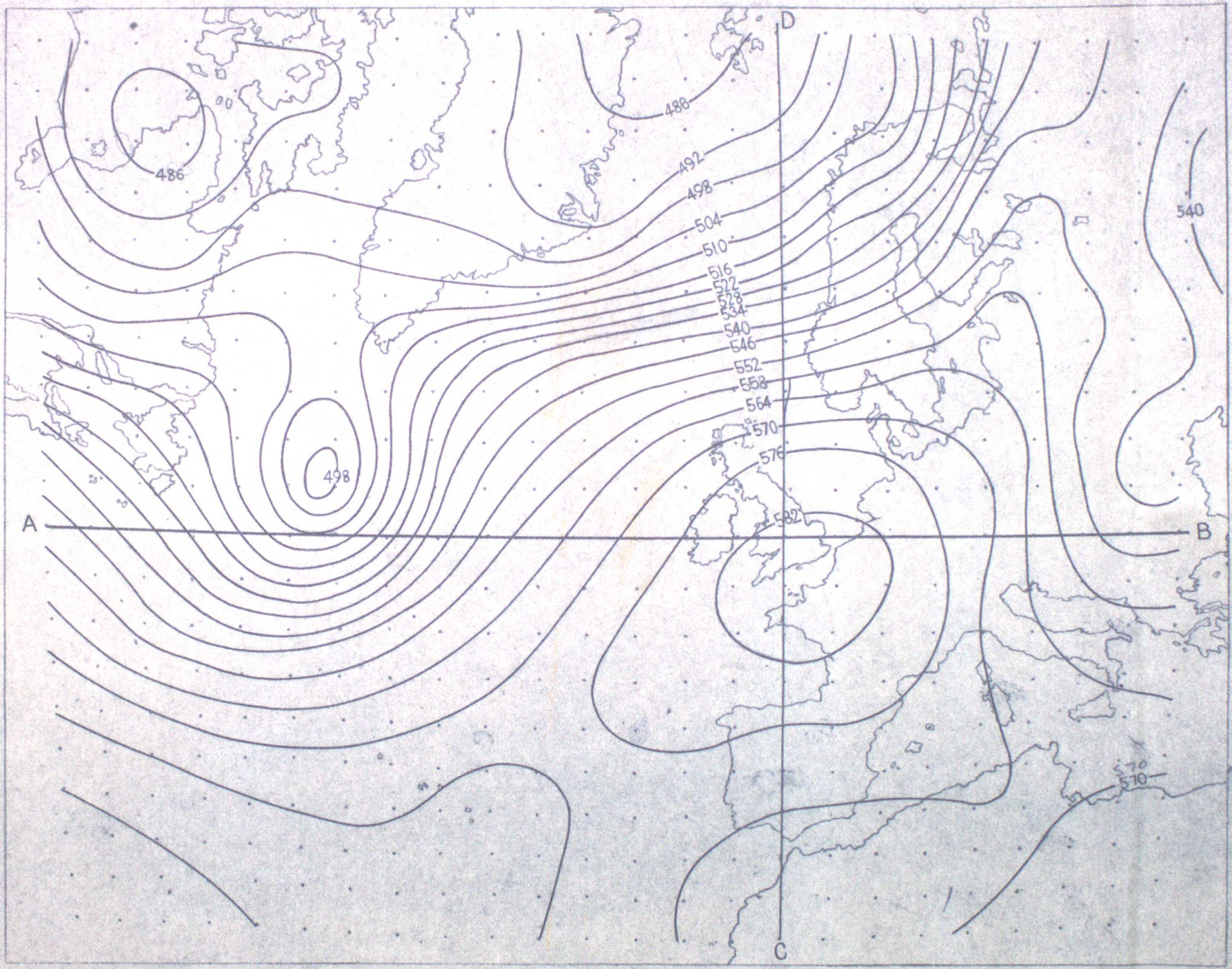

Fig. 5(b) 500 mb. contours 17 Feb. 1959

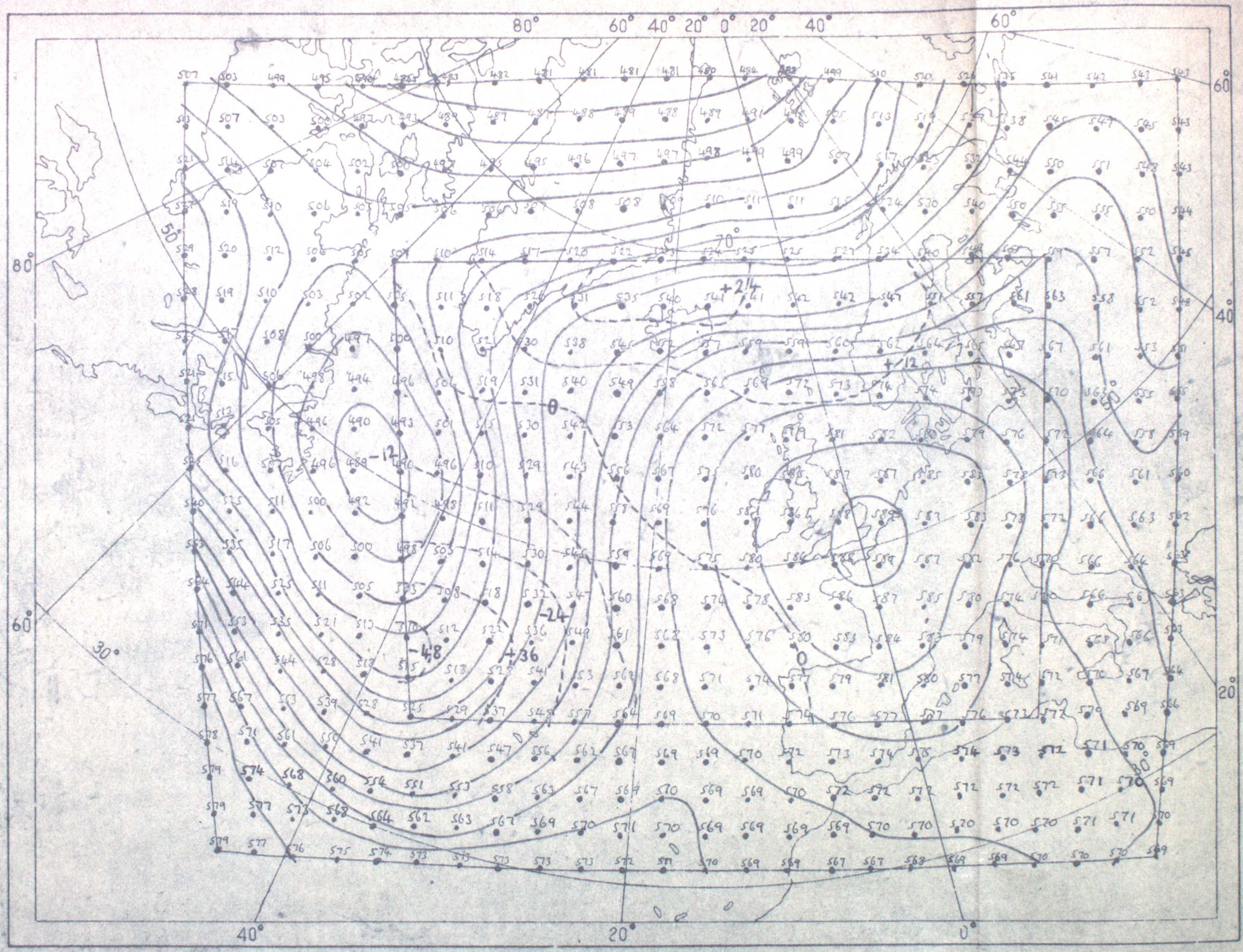

BIL (I)

500 MB 16-2-59

Fig. 5(c) Forecast for 0000 G.M.T. 17.2.59 based on 0000 G.M.T 16.2.59

Printed by Air Ministry P.R.B.

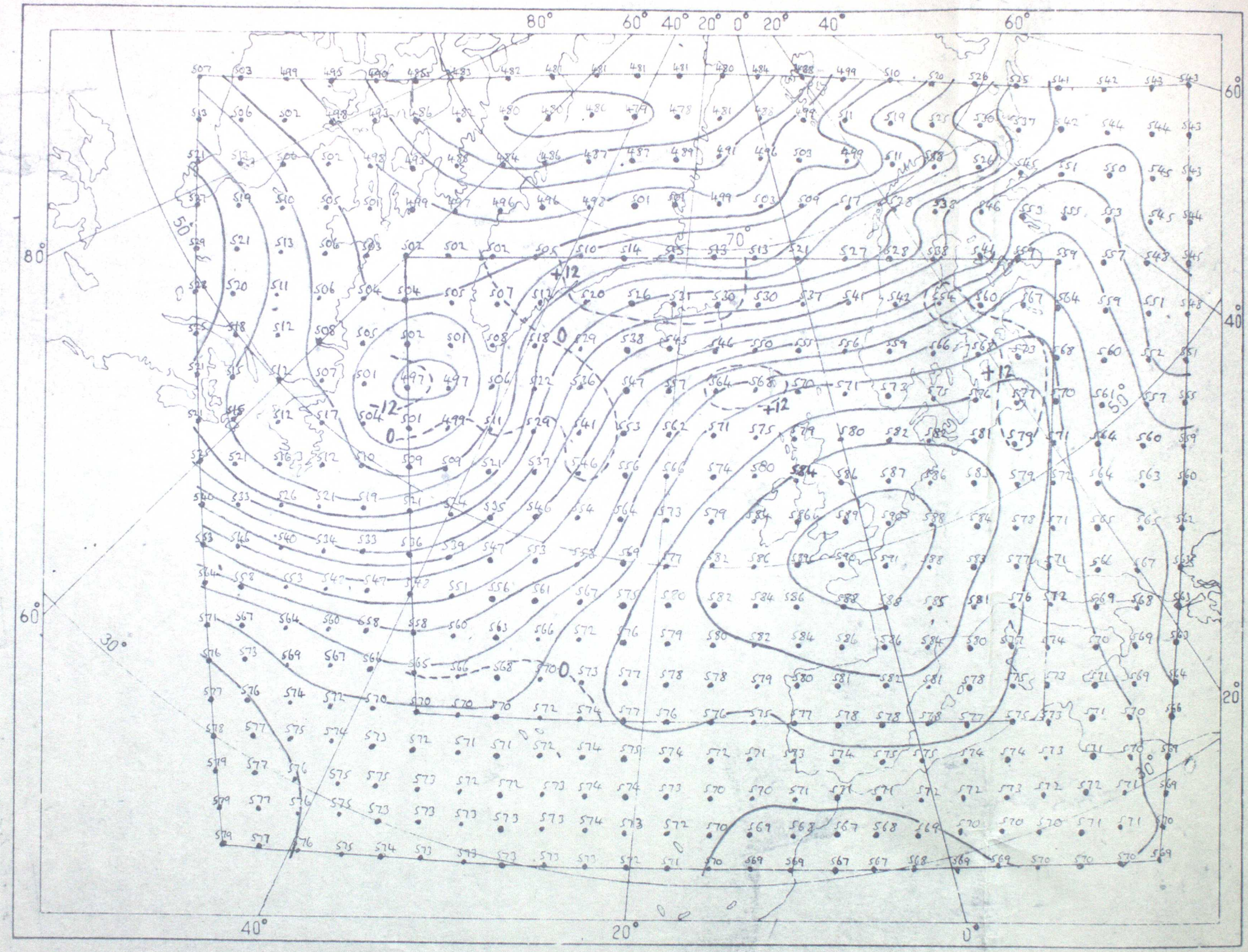

BIX

500 MB 16-2-59

Fig. 5(d) Forecast for 0000 G.M.T. 17.2.59, based on 0000 G.M.T 16.2.59

Printed by Air Ministry P.R.B

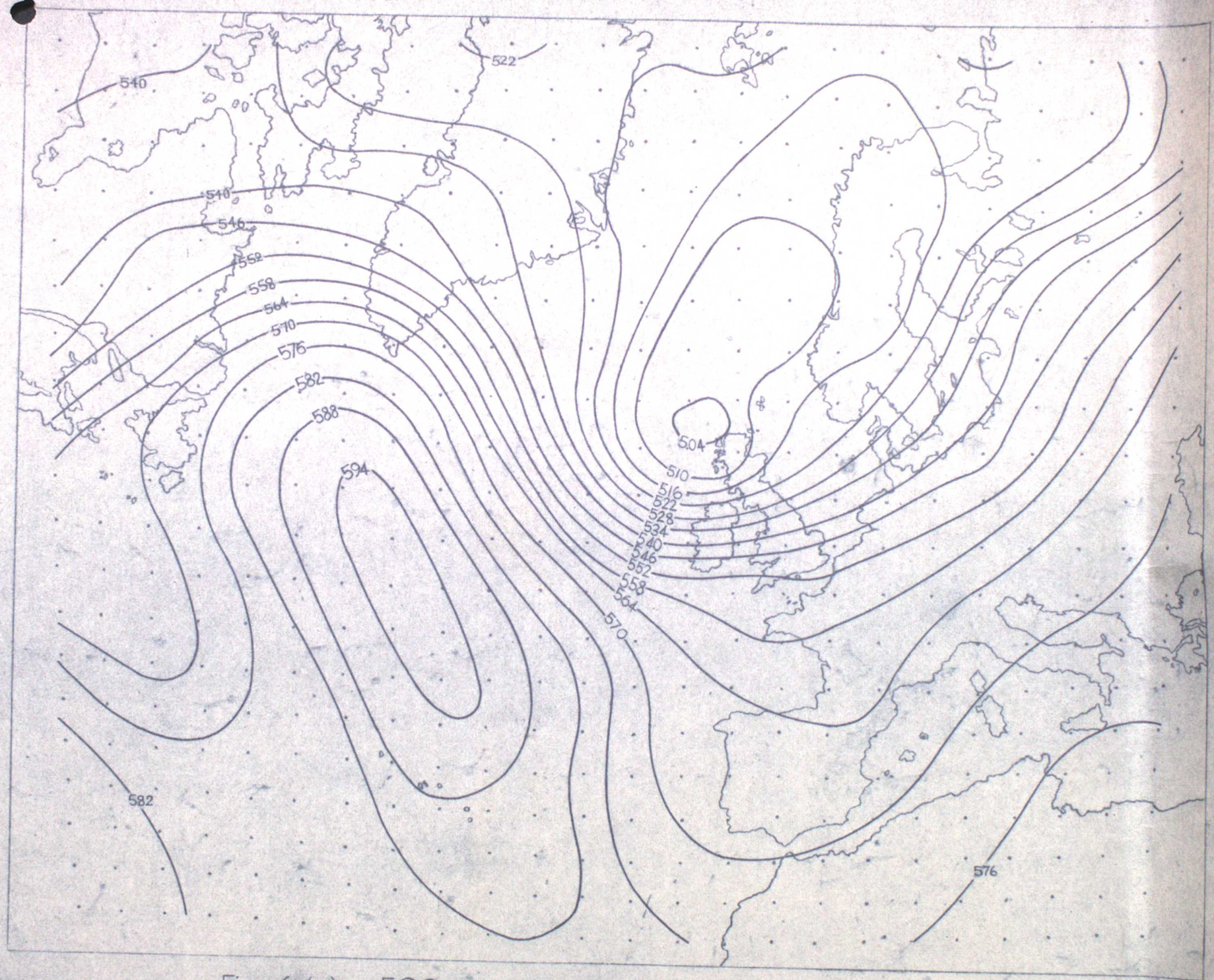

Fig. 6 (a) 500 mb. contours 27 Oct 1959

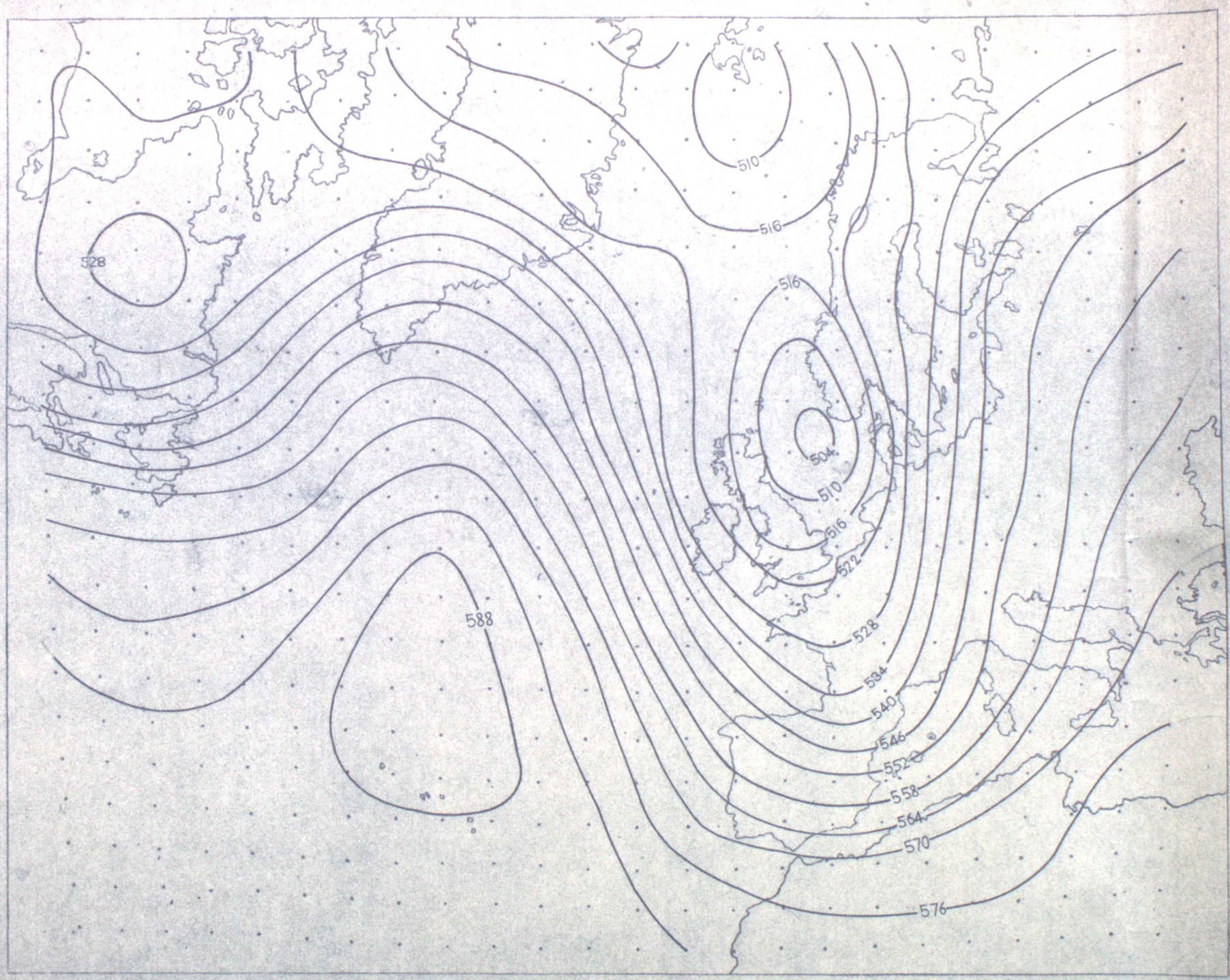

Fig. 6 (b) 500mb. contours 28 Oct. 1959

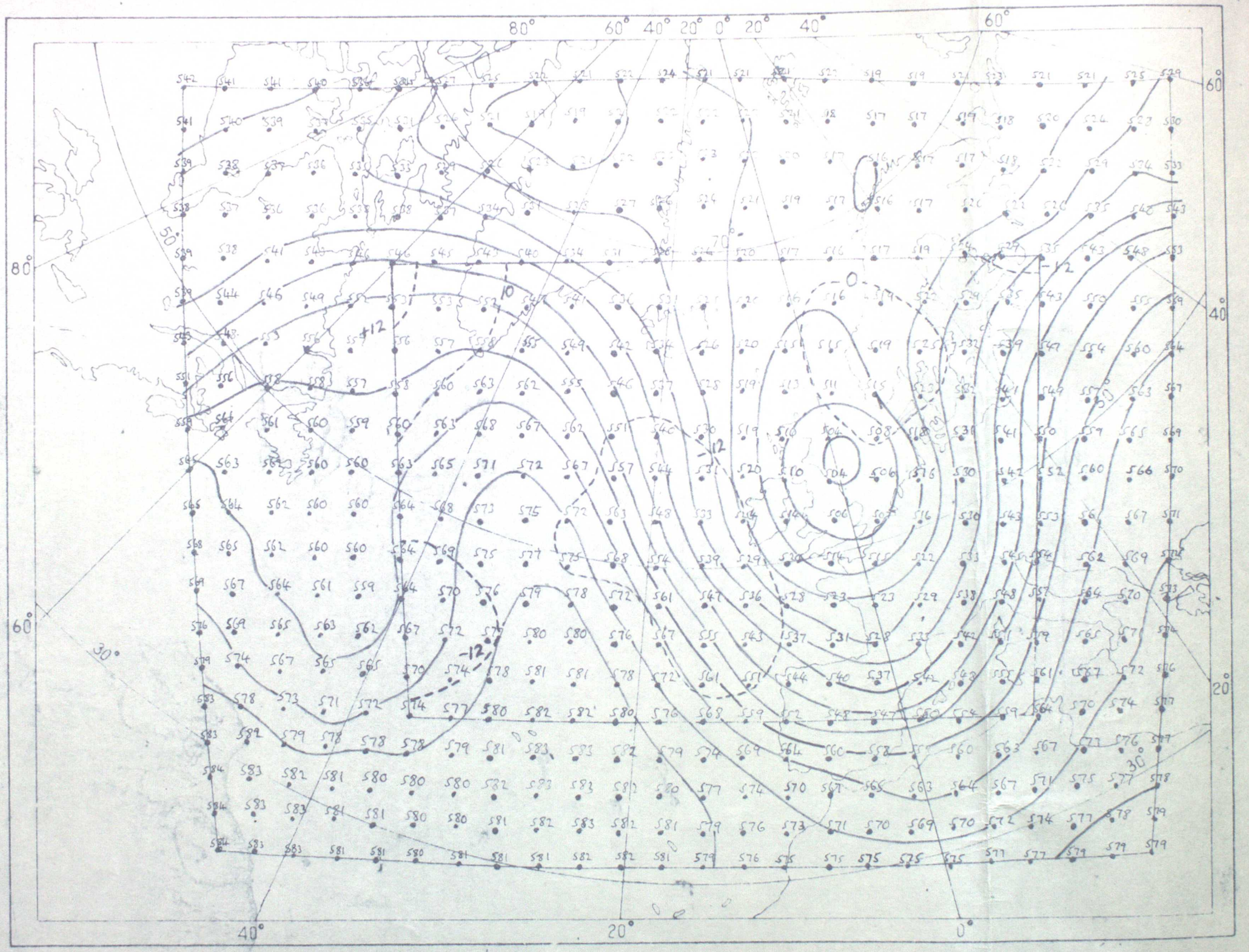

Fig. 6 (c) Forecast for 0000 G.M.T. 28.10.59 based on 0000 G.M.T. 27.10.59

BIL (I)
500 MB 27-10-59

Printed by Air Ministry P.R.B

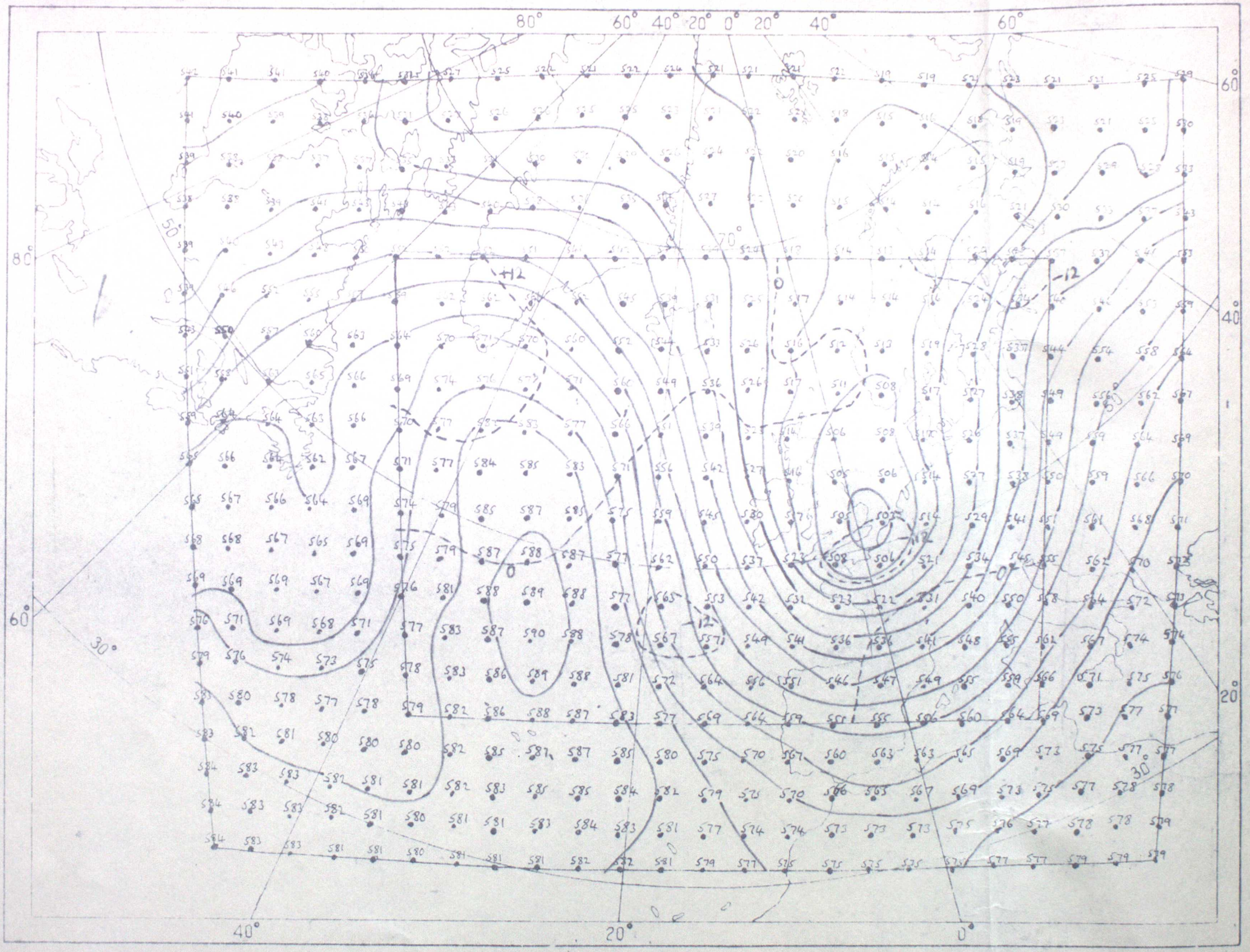

BIX

500 MB 27-10-59

Fig 6(d) Forecast for 0000 G.M.T. 28.10.59, based on 0000 G.M.T 27.10.59

Printed by Air Ministry P.R.B.